

# Description of $^{178}\text{Hf}^{m2}$ in the constrained relativistic mean field theory \*

ZHANG Wei<sup>†,1,2</sup> PENG Jing,<sup>3</sup> and ZHANG Shuang-Quan<sup>1</sup>

<sup>1</sup>*School of Physics, and State Key Laboratory of Nuclear Physics and Technology, Peking University, Beijing 100871*

<sup>2</sup>*School of Electrical Engineering and Automation, He'nan Polytechnic University, Jiaozuo 454003*

<sup>3</sup>*Department of Physics, Beijing Normal University, Beijing 100875*

(Dated: November 5, 2018)

## Abstract

The properties of the ground state of  $^{178}\text{Hf}$  and the isomeric state  $^{178}\text{Hf}^{m2}$  are studied within the adiabatic and diabatic constrained relativistic mean field (RMF) approaches. The RMF calculations reproduce well the binding energy and the deformation for the ground state of  $^{178}\text{Hf}$ . Using the ground state single-particle eigenvalues obtained in the present calculation, the lowest excitation configuration with  $K^\pi = 16^+$  is found to be  $\nu(7/2^- [514])^{-1}(9/2^+ [624])^1 \pi(7/2^+ [404])^{-1}(9/2^- [514])^1$ . Its excitation energy calculated by the RMF theory with time-odd fields taken into account is equal to 2.801 MeV, i.e., close to the  $^{178}\text{Hf}^{m2}$  experimental excitation energy 2.446 MeV. The self-consistent procedure accounting for the time-odd component of the meson fields is the most important aspect of the present calculation.

PACS numbers: 21.10.-k, 21.60.-n, 27.70.+q

---

\* Supported by the National Natural Science Foundation of China under Grant Nos 10605004 and 10705004, the Natural Science Foundation of He'nan Educational Committee under Grant No 200614003, and the Young Backbone Teacher Support Program of He'nan Polytechnic University

<sup>†</sup> Email: zw76@pku.org.cn

The relativistic mean-field (RMF) theory is one of the most successful microscopic models in nuclear physics. [1, 2, 3] From the very beginning, it incorporates the important relativistic effects, and it has achieved success in describing many nuclear phenomena related to stable nuclei [2, 3], exotic nuclei [4, 5] as well as supernova and neutron stars [6]. The RMF theory provides a new explanation for the identical bands in superdeformed nuclei [7] and for the neutron halo in heavy nuclei [4], it predicts giant neutron halos, a new phenomenon in heavy nuclei close to the neutron drip line [5, 8], it naturally generates the spin-orbit potential, explains the origin of the pseudospin symmetry as a relativistic symmetry [9, 10, 11], and spin symmetry in the anti-nucleon spectrum [12], and also describes well the magnetic rotation [13], the collective multipole excitations [14] as well as the properties of hypernuclei [15], etc. Lately, the ground state properties of about 7000 nuclei have been calculated in the RMF+BCS model and good agreements with existing experimental data were obtained [16]. Recent and more complete reviews of the applications of the RMF model, particularly, those to exotic nuclei, can be found in Refs. [17, 18] .

Recently the 31-yr isomer of  $^{178}\text{Hf}$  (also called  $^{178}\text{Hf}^{m2}$ ,  $K^\pi = 16^+$ ,  $E_x=2.446\text{MeV}$ ) has attracted extensive attention [19, 20, 21, 22, 23] for its potential to be a good medium of energy storage [24]. The long half-life of  $^{178}\text{Hf}^{m2}$  is connected with the strong inhibition of spontaneous electromagnetic transitions restricted by the  $K$  selection rule, and it supports the point of view that this high- $K$  state has an axially symmetric intrinsic shape [22]. The configuration originally suggested for the isomer  $^{178}\text{Hf}^{m2}$  is  $\nu^2(7/2^- [514])(9/2^+ [624])\pi^2(7/2^+ [404])(9/2^- [514])$  [25], which was further supported by the view of alignment and by the  $g$ -factor of the corresponding rotation bands. [26]

In this Letter, we will study the properties of the ground state of  $^{178}\text{Hf}$  and also investigate the possible configuration of  $^{178}\text{Hf}^{m2}$  within the self-consistent axially symmetric RMF theory. From the point of views of the adiabatic constrained calculation, nuclear ground state presents the global minimum of the potential energy surface (PES). To study the excited states, like isomers, the diabatic (configuration-fixed) constrained approach can be applied as an effective method. [27] Within the adiabatic constrained approach, nucleons always occupy the lowest levels, while in the diabatic constrained approach, the configuration is kept fixed by the so-called concept of “parallel transport”. In the present paper, both the adiabatic and diabatic constrained RMF approaches are applied in our investigation.

The basic ansatz of the RMF theory is a Lagrangian density where nucleons are described

as Dirac particles which interact via the exchange of various mesons and the photon. The mesons considered are the isoscalar-scalar  $\sigma$ , the isoscalar-vector  $\omega$  and the isovector-vector  $\rho$ . The effective Lagrangian density reads <sup>[1]</sup>

$$\begin{aligned}
\mathcal{L} = & \bar{\psi} \left[ i\gamma^\mu \partial_\mu - M - g_\sigma \sigma - g_\omega \gamma^\mu \omega_\mu - g_\rho \gamma^\mu \vec{\tau} \cdot \vec{\rho}_\mu - e\gamma^\mu \frac{1 - \tau_3}{2} A_\mu \right] \psi \\
& + \frac{1}{2} \partial^\mu \sigma \partial_\mu \sigma - \frac{1}{2} m_\sigma^2 \sigma^2 - \frac{1}{3} g_2 \sigma^3 - \frac{1}{4} g_3 \sigma^4 \\
& - \frac{1}{4} \Omega^{\mu\nu} \Omega_{\mu\nu} + \frac{1}{2} m_\omega^2 \omega^\mu \omega_\mu + \frac{1}{4} c_3 (\omega^\mu \omega_\mu)^2 \\
& - \frac{1}{4} \vec{R}^{\mu\nu} \cdot \vec{R}_{\mu\nu} + \frac{1}{2} m_\rho^2 \vec{\rho}^\mu \cdot \vec{\rho}_\mu \\
& - \frac{1}{4} F^{\mu\nu} F_{\mu\nu}
\end{aligned} \tag{1}$$

in which the field tensors for the vector mesons and the photon are, respectively, defined as

$$\begin{cases} \Omega_{\mu\nu} = \partial_\mu \omega_\nu - \partial_\nu \omega_\mu, \\ \vec{R}_{\mu\nu} = \partial_\mu \vec{\rho}_\nu - \partial_\nu \vec{\rho}_\mu, \\ F_{\mu\nu} = \partial_\mu A_\nu - \partial_\nu A_\mu. \end{cases} \tag{2}$$

From the Lagrangian, the equation of motion for the nucleon is

$$\{ \boldsymbol{\alpha} \cdot [-i\nabla - \mathbf{V}(\mathbf{r})] + V_0(\mathbf{r}) + \beta[M + S(\mathbf{r})] \} \psi_i = \varepsilon_i \psi_i, \tag{3}$$

with the attractive scalar potential  $S(\mathbf{r}) = g_\omega \omega(\mathbf{r})$ , the usual repulsive vector potential  $V_0(\mathbf{r}) = g_\omega \omega_0(\mathbf{r}) + g_\rho \tau_3 \rho_0(\mathbf{r}) + e \frac{1 - \tau_3}{2} A_0(\mathbf{r})$ , and the nuclear magnetic potential  $\mathbf{V}(\mathbf{r}) = g_\omega \boldsymbol{\omega}(\mathbf{r}) + g_\rho \tau_3 \boldsymbol{\rho}(\mathbf{r}) + e \frac{1 - \tau_3}{2} \mathbf{A}(\mathbf{r})$ . The Klein-Gordon equations for the mesons and electromagnetic fields are

$$(-\nabla^2 + m_\zeta^2) \zeta(\mathbf{r}) = S_\zeta(\mathbf{r}), \tag{4}$$

where  $S_\zeta(\mathbf{r})$  is the source term and all other notations are the same as in Ref. [18].

In the RMF approaches which are widely used, only the time-even fields are essential for the physical observables, since the time-odd components of vector fields do not exist because of the time reversal symmetry for the ground state of an even-even nucleus. For an odd- $A$  or odd-odd nucleus, the unpaired valence nucleon will give non-vanishing contribution to the nuclear current which provides the time-odd component of vector fields, i.e., the nuclear

magnetic potential. It is found that the nuclear magnetic potential has small influence on the root-mean-square radii and quadrupole moments while it plays an important role in the single-particle properties and magnetic moments in odd- $A$  or odd-odd nuclei.<sup>[28, 29]</sup> One should keep in mind that for the excited states in the even-even nuclei, there may also exist the unpaired nucleons, which result in non-vanishing time-odd field. Therefore the time-odd fields should also be treated carefully for some isomeric states in the even-even nuclei, as in the odd- $A$  or odd-odd nuclei. In the calculation without current, the nuclear magnetic potential  $\mathbf{V}(\mathbf{r})$  will be neglected.

For the adiabatic constrained approach, the binding energy at a certain deformation is obtained by constraining the mass quadrupole moment  $\langle \hat{Q}_2 \rangle$  to a given value  $\mu$ , i.e.

$$\langle H' \rangle = \langle H \rangle + \frac{1}{2}C(\langle \hat{Q}_2 \rangle - \mu)^2. \quad (5)$$

where  $C$  is the curvature constant parameter, and  $\mu$  is the given quadrupole moment. The expectation value of  $\hat{Q}_2$  is  $\langle \hat{Q}_2 \rangle = \langle \hat{Q}_2 \rangle_n + \langle \hat{Q}_2 \rangle_p$ , where  $\langle \hat{Q}_2 \rangle_{n,p} = \langle 2r^2 P_2(\cos \theta) \rangle_{n,p}$ . The deformation parameter  $\beta_2$  is related to  $\langle \hat{Q}_2 \rangle$  by  $\langle \hat{Q}_2 \rangle = \frac{3}{\sqrt{5\pi}} Ar^2 \beta_2$ ,  $r = R_0 A^{1/3}$  ( $R_0 = 1.2$  fm) and  $A$  is the mass number. By varying  $\mu$ , the binding energy at different deformations can be obtained<sup>[30]</sup>.

For the adiabatic constrained approach, the occupied levels are determined by the so-called ‘‘parallel transport’’<sup>[27]</sup>, i.e.,

$$\langle \psi_i(q) | \psi_j(q + \Delta q) \rangle |_{\Delta q \rightarrow 0} \approx \delta_{ij}, \quad (6)$$

where  $i$  and  $j$  enumerate all the single-particle levels of two adjacent configurations. In such a way, the original configuration at  $q$  can be traced and the corresponding PES can be obtained as a function of the deformation<sup>[27]</sup>. In principle, if  $\Delta q$  is small enough, the configurations at  $q$  and at  $q + \Delta q$  should be the same. In the calculation, the two-step procedure is adopted: first, the wave functions and the configuration at the initial  $q$  are recorded. Second, the wave functions  $|\psi_i(q)\rangle$  are mapped to  $|\psi_j(q + \Delta q)\rangle$  one by one by searching the largest overlap in  $|\psi_j(q + \Delta q)\rangle$  with the same quantum number  $\Omega^\pi$ . The configuration is transferred by copying the occupation number from  $|\psi_i(q)\rangle$  to the mapped  $|\psi_j(q + \Delta q)\rangle$ . The wave functions and the configuration at this  $q + \Delta q$  are also recorded. The second step is repeated until enough points on the diabatic PES are obtained.

The constrained RMF calculations are carried out with parameter set PK1<sup>[31]</sup>. The full  $N = 20$  deformed harmonic-oscillator shells for fermions and bosons are taken into account

as the basis. This basis is large enough to produce a converged binding energy at certain deformation.

The PES of  $^{178}\text{Hf}$  obtained in adiabatic (open circles) and diabatic (lines) constrained RMF calculations are plotted in Fig. 1. The calculated energy  $E=-1434.0$  MeV and the deformation  $\beta_2=0.283$  of the ground state (denoted as a black asterisk in Fig. 1) are in good agreement with the experimental energy  $-1432.8$  MeV <sup>[32]</sup> and deformation  $0.280$  <sup>[33]</sup>. In this figure, the adiabatic PES can be decomposed into three regions by the discontinuity, i.e.,  $\beta_2=0.22 \sim 0.32$  (region 1),  $\beta_2 = 0.35 \sim 0.40$  (region 2),  $\beta_2 = 0.43 \sim 0.50$  (region 3). It is known that the discontinuity originates from the change of the configurations, and the configuration for all points in one region is the same. This is confirmed by the diabatic constrained calculation in which the configuration is kept fixed during the constraint procedure. It can be seen in Fig. 1 that for every region the diabatic calculation (solid curves) coincides with the adiabatic calculation (open circles) and extends the region much wider. The crossover of the solid curves announces the change of the configurations. For example, from region 1 to region 2, the configuration changes from the ground state to  $\pi(7/2^+[404])^{-2}(1/2^-[541])^2$ , where microscopically the proton level  $7/2^+[404]$  below the Fermi surface in region 1 becomes unoccupied while the proton level  $1/2^-[541]$  above the Fermi surface in region 1 becomes occupied. Since a pair of protons change the levels at the same time, the  $K$ -values remain zero for region 2. Similarly, from region 2 to region 3, the configuration changes from  $\pi(7/2^+[404])^{-2}(1/2^-[541])^2$  to  $\nu(5/2^-[512])^{-2}(1/2^+[660])^2\pi(7/2^+[404])^{-2}(1/2^-[541])^2$  and the  $K$ -values also remain zero for region 3.

Based on the single-particle spectra of the ground state, one can construct excited states with high  $K$ -values. In a deformed, axially symmetric nucleus, a high- $K$  state is made by summing the contributions from several unpaired quasiparticles. To form low-lying high- $K$  states, several high- $\Omega$  single-particle (both neutron and proton) levels lying close to the Fermi surface are necessary. The well-deformed nuclei with  $A \approx 180$ , including  $^{178}\text{Hf}$ , satisfy this requirement very well. With the restriction of the total  $\Omega$  and parity as  $16^+$ , the candidate configurations of  $^{178}\text{Hf}^{m2}$  will be constructed.

For the ground state of  $^{178}\text{Hf}$ , the neutron (proton) single-particle levels close to the Fermi surface are shown in the first column of the left (right) panel in Fig. 2. Each level is labeled by the Nilsson notation  $\Omega^\pi[Nn_zm_l]$  of its main component. It can be seen that in Fig. 2, the energy required to excite one neutron or one proton is not less than 0.63 or 1.84

MeV. As the experimental excitation energy of  $^{178}\text{Hf}^{m2}$  equals 2.446 MeV, it is sufficient to consider one- or two-neutron excitations, together with one- or two-proton excitations. For two-neutron (two-proton) excitations, the following cases are considered: in the first case, a pair of particles below the Fermi surface are excited to two different levels above the Fermi surface; in the other case, two particles occupying different levels below the Fermi surface are excited to form a new pair. Those cases which involve four or more single-particle levels are not included for simplicity. All possible configurations are constructed by restricting the  $K$  (total  $\Omega$ ) value to 16 and the nuclear parity to  $+$ . Thus the configurations with the lowest excitation energies are obtained and labeled by  $16_1^+$ ,  $16_2^+$ ,  $16_3^+$ , etc.

The detailed configurations of the five lowest  $K^\pi = 16^+$  states of  $^{178}\text{Hf}$  are listed in column 2 of Table I. In this table, the first 4 states are one-neutron plus one-proton excitation, while the last one is a pair of neutrons excited to high- $\Omega$  levels combined with the one-proton excitation. The configuration of  $16_1^+$  is  $\nu(7/2^-[514])^{-1}(9/2^+[624])^1 \pi(7/2^+[404])^{-1}(9/2^-[514])^1$  with respect to the ground state, i.e., one formerly paired neutron in the level  $7/2^-[514]$  becomes unpaired and excited to the level  $9/2^+[624]$ , and another formerly paired proton in level  $7/2^+[404]$  is excited to the level  $9/2^-[514]$ . This configuration is consistent with the former assignment of  $^{178}\text{Hf}^{m2}$  [25, 26]. Note that the excitation energy of  $16_1^+$  given by the sum of single particle excitations is 3.954 MeV which is about 1.5 MeV higher than the experimental value 2.446 MeV.

In order to obtain the self-consistent excitation energy for state  $16_1^+$  microscopically, the diabatic constrained RMF calculations are carried out with the respective configuration information. As discussed before, the time-odd fields [29] caused by the unpaired nucleons should be taken into account carefully for the high- $K$  state. The time-even calculation is also done for comparison. The PES of state  $16_1^+$  with (without) current is plotted as a solid (dashed) red curve in Fig. 1, together with the PES of state  $16_2^+$ . The local minima of  $16_1^+$  ( $16_2^+$ ) PES are denoted as up (down) triangles in Fig. 1. For state  $16_1^+$ , the excitation energy according to the calculations without and with current is, respectively 3.579 MeV and 2.801 MeV, which clearly shows that both the self-consistent calculation and the consideration of the time-odd fields are crucial effects to obtain the reasonable excitation energy. The excitation energy of  $16_1^+$  ( $E_x = 2.801$  MeV) is close to the experimental excitation energy ( $E_x = 2.446$  MeV) of  $^{178}\text{Hf}^{m2}$ . The deformation ( $\beta_2 = 0.30$ ) obtained for this isomer is similar to that of the ground state. In Table I, all the excitation energies from calculations without

and with current as well as the deformation calculated for the states  $16_1^+$  to  $16_5^+$  are also given. For all five states, the excitation energies calculated with current are 0.6 ~0.8MeV smaller than those without current. By the way, the same approaches are also applied to the isomeric state  $^{178}\text{Hf}^m$  (experimentally  $K^\pi=8^-, E_x=1.147\text{MeV}$ ). The configuration obtained for  $8_1^-$  is  $\pi(7/2^+[404])^{-1}(9/2^-[514])^1$ , and the excitation energy without and with current is, respectively 1.552 MeV and 1.315 MeV.

In Fig. 2, the neutron and proton single-particle levels of state  $16_1^+$  from the RMF without and with current have been plotted in columns 2, 3 in both panels. In the time-odd calculation each single-particle level splits into two levels due to the breaking of the time-reversal symmetry, the level with positive  $\Omega$  being energetically favored. Such splittings will change straightforward the energy gap between two single-particle levels. In particular, for one-neutron and one-proton excitation of the state  $16_1^+$  discussed here, the neutron energy gap between  $\nu(9/2^+[624])$  and  $\nu(7/2^-[514])$  in the calculation without current decreases from 2.00 MeV to 1.25 MeV, which is the gap between  $\nu(9/2^+[624], +\Omega)$  and  $\nu(7/2^-[514], -\Omega)$  in the calculation with current. Correspondingly the energy gap for the proton excitation concerned decreases from 1.34 MeV to 0.54 MeV. As a result, the calculation with current decreases the excitation energy considerably.

In summary, the properties of the ground state of  $^{178}\text{Hf}$  and the isomeric state  $^{178}\text{Hf}^{m2}$  are investigated by the adiabatic and diabatic constrained RMF approaches. The constrained RMF theory reproduces well the binding energy and deformation for the ground state of  $^{178}\text{Hf}$ . With the single-particle levels of the ground state obtained in the adiabatic constrained RMF theory, by restricting  $K^\pi = 16^+$ , the configuration with the lowest excitation energy is found to be  $\nu(7/2^-[514])^{-1}(9/2^+[624])^1 \pi(7/2^+[404])^{-1}(9/2^-[514])^1$ , which is consistent with the former configuration assignment. The excitation energy based on the single-particle spectra is 3.954 MeV, which is much higher than the experimental excitation energy 2.446 MeV of  $^{178}\text{Hf}^{m2}$ . By applying the self-consistent time-even and time-odd RMF calculation, the excitation energy of this configuration is decreased to 3.579 MeV and 2.801 MeV, respectively. Therefore both the self-consistency and the consideration of current are important factors for studying nuclear isomers.

The authors gratefully acknowledge Professor Jie Meng, Professor L. N. Savushkin, and

Dr. Jiangming Yao for their helpful suggestions and discussions.

---

- [1] Serot B D and Walecka J D 1986 *Adv. Nucl. Phys.* **16** 1
- [2] Reinhard P -G 1989 *Rep. Prog. Phys.* **52** 439
- [3] Ring P 1996 *Prog. Part. Nucl. Phys.* **37** 193
- [4] Meng J and Ring P 1996 *Phys. Rev. Lett.* **77** 3963
- [5] Meng J and Ring P 1998 *Phys. Rev. Lett.* **80** 460
- [6] Glendenning N K 2000 *Compact Stars* (Springer-Verlag, New York)
- [7] König J and Ring P 1993 *Phys. Rev. Lett.* **71** 3079
- [8] Meng J, Toki H, Zeng J Y, Zhang S Q and Zhou S G 2002 *Phys. Rev. C* **65** 8041302
- [9] Ginocchio J N 1997 *Phys. Rev. Lett.* **78** 436
- [10] Meng J, Sugawara-Tanabe K, Yamaji S, Ring P and Arima A 1998 *Phys. Rev. C* **58** 8628
- [11] Meng J, Sugawara-Tanabe K, Yamaji S and Arima A 1999 *Phys. Rev. C* **59** 154
- [12] Zhou S G, Meng J and Ring P 2003 *Phys. Rev. Lett.* **91** 262501
- [13] Madokoro H, Meng J, Matsuzaki M and Yamaji S 2000 *Phys. Rev. C* **62** 061301
- [14] Ma Z Y, Wandelt A, Giai N V, Vretenar D, Ring P and Cao L G 2002 *Nucl. Phys. A* **703** 222
- [15] Mares J and Jennings B K 1994 *Phys. Rev. C* **49** 2472
- [16] Geng L S, Toki H and Meng J 2005 *Prog. Theor. Phys.* **113** 785
- [17] Vretenar D, Afanasiev A V, Lalazissis G A and Ring P 2005 *Phys. Rep.* **409** 101
- [18] Meng J, Toki H, Zhou S G, Zhang S Q, Long W H and Geng L S 2006 *Prog. Part. Nucl. Phys.* **57** 470
- [19] Hayes A B et al 2002 *Phys. Rev. Lett.* **89** 242501
- [20] Cline D, Hayes A B and Wu C Y 2005 *Journal of Modern Optics* **52(16)** 2411
- [21] Hayes A B et al 2007 *Phys. Rev. C* **75** 034308
- [22] Sun Y, Zhou X-R, Long G-L, Zhao E-G and Walker P 2004 *Phys. Lett. B* **589** 83
- [23] Tu Y, Chen Y-S and Gao Z-C 2006 *High Energy Phys. Nucl. Phys. Suppl.2* **30** 109
- [24] Collins C B et al 1999 *Phys. Rev. Lett.* **82** 695
- [25] Helmer R G and Reich C W 1968 *Nucl. Phys. A* **114** 649
- [26] Mullins S M, Dracoulis G D, Byrne A P, et al 1997 *Phys. Lett. B* **393** 279

- [27] Lü H F, Geng L S and Meng J 2007 *Eur. Phys. J. A* **31** 273
- [28] Warriar Latha S and Gambhir Y K 1994 *Phys. Rev. C* **49** 871
- [29] Yao J M, Chen H and Meng J 2006 *Phys. Rev. C* **74** 024307
- [30] Ring P and Schuck P 1980 *The Nuclear Many-body Problem* (New York:Springer-Verlag) 269
- [31] Long W H, Meng J, Giai N V and Zhou S G 2004 *Phys. Rev. C* **69** 034319
- [32] Audi G, Wapstra A H and Thibault C 2003 *Nucl. Phys. A* **729** 337
- [33] Raman S, Nestor C W, JR and Tikkanen P 2001 *At. Data Nucl. Data Tables* **78** 1

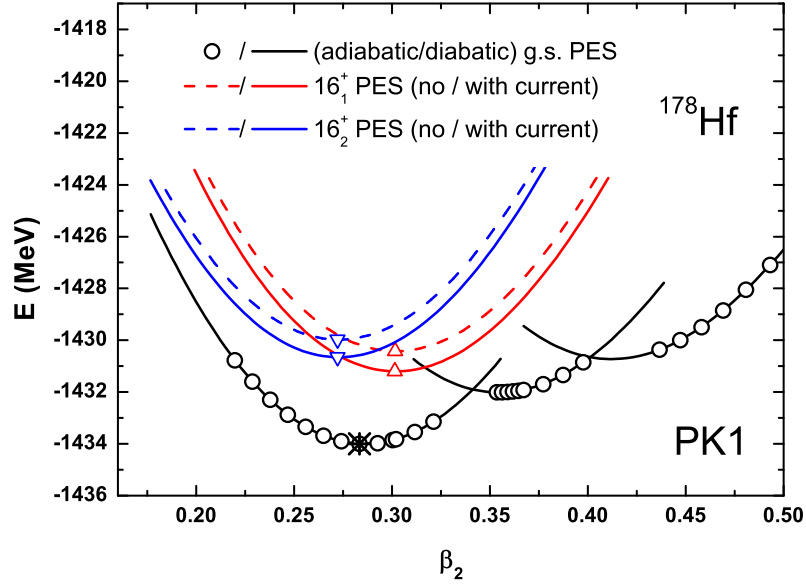


FIG. 1: (color online) Potential energy surfaces (PES) of  $^{178}\text{Hf}$  from adiabatic (open circles) and diabatic (solid curves) RMF calculations, as well as the PES of the first two  $16^+$  states  $16_1^+$  (red) and  $16_2^+$  (blue) from the adiabatic constrained RMF calculations with (solid curves) and without (dashed curves) current. The RMF parameter set PK1 is adopted. The ground state as well as the local minima  $16_1^+$  ( $16_2^+$ ) are denoted as a black asterisk and red (blue) triangles, respectively.

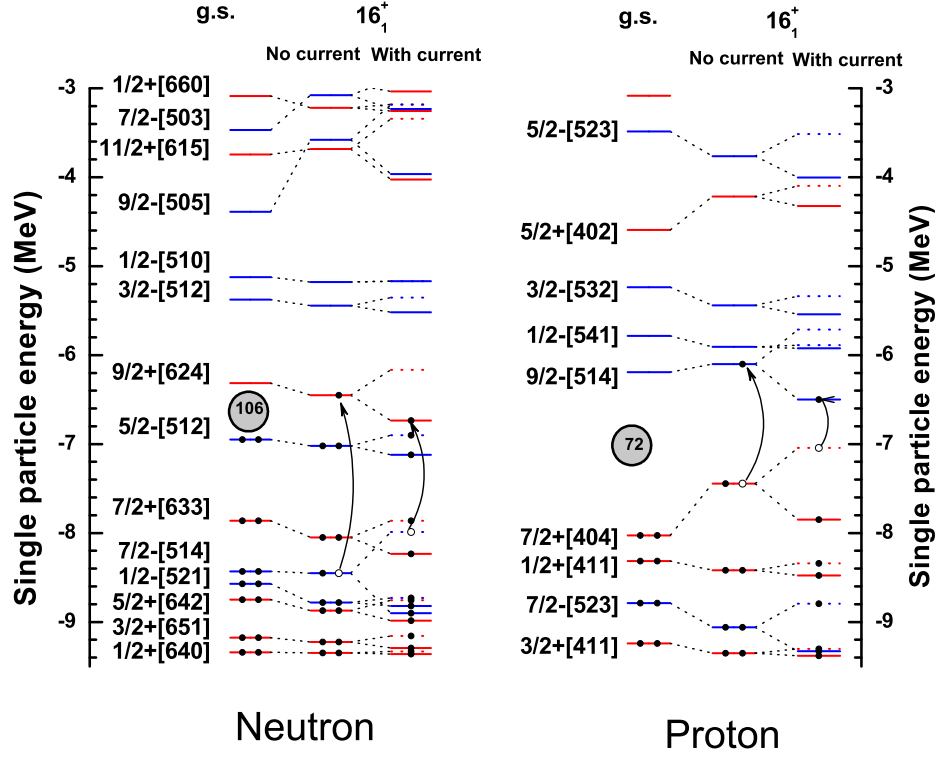


FIG. 2: (color online) Neutron (left panel) and proton (right panel) single-particle levels of the ground states (1st column), state  $16_1^+$  of  $^{178}\text{Hf}$  obtained from the constrained RMF approach without (2nd column) and with (3rd column) current. Each level is labeled by the Nilsson notation  $\Omega\pi[Nn_zm_l]$  of its main component. The Fermi surfaces are marked by neutron and proton numbers in the grey circles. The red (blue) lines denote the parity + (-), and the dashed (solid) lines denote the positive (negative) signs of  $\Omega$ , respectively. The configuration difference is illustrated by filled circles, open circles and arrows.

TABLE I: The configurations, excitation energies as well as the deformations obtained from the adiabatic and diabatic constrained RMF approaches for the first five  $K^\pi = 16^+$  states of  $^{178}\text{Hf}$ . The excitation energies (in MeV) include the sum of single-particle excitations  $\sum(\varepsilon_j - \varepsilon_i)$ , and the excitation energies  $E_x$  calculated without (with) current.

State	Configuration	$\sum(\varepsilon_j - \varepsilon_i)$	$E_x$ (no current)	$E_x$ (with current)	$\beta_2$ (with current)
$16_1^+$	$\nu(7/2^- [514])^{-1}(9/2^+ [624])^1$	2.119	3.954	3.579	2.801
	$\pi(7/2^+ [404])^{-1}(9/2^- [514])^1$	1.835			
$16_2^+$	$\nu(7/2^+ [633])^{-1}(9/2^+ [624])^1$	1.549	4.146	4.025	3.342
	$\pi(7/2^- [523])^{-1}(9/2^- [514])^1$	2.597			
$16_3^+$	$\nu(5/2^- [512])^{-1}(11/2^+ [615])^1$	3.204	5.039	4.749	4.129
	$\pi(7/2^+ [404])^{-1}(9/2^- [514])^1$	1.835			
$16_4^+$	$\nu(7/2^+ [633])^{-1}(9/2^- [505])^1$	3.473	5.308	5.380	4.601
	$\pi(7/2^+ [404])^{-1}(9/2^- [514])^1$	1.835			
$16_5^+$	$\nu(5/2^- [512])^{-2}(9/2^+ [624])^1(7/2^- [503])^1$	4.113	5.948	5.879	5.302
	$\pi(7/2^+ [404])^{-1}(9/2^- [514])^1$	1.835			